



AIAA-90-3965

**Noise Transmission of a Large Scale
Composite Fuselage Model**

T. Beyer and R. Silcox, NASA-Langley,
Hampton, VA

AIAA 13th Aeroacoustics Conference

October 22-24, 1990 / Tallahassee, FL

NOISE TRANSMISSION CHARACTERISTICS OF A LARGE SCALE COMPOSITE FUSELAGE MODEL

Todd B. Beyer and Richard J. Silcox
NASA Langley Research Center
Hampton, VA 23665-5225

Abstract

A study of the basic noise transmission characteristics of a realistic, built-up composite fuselage model is described. A floor-equipped, stiffened composite cylinder, 5.5 feet in diameter and 12 feet in length was mounted on a stand in a large anechoic chamber and exposed to several different exterior noise source configurations. The exterior source configurations studied include a single point source, two point sources located in the same plane on opposite sides of the cylinder operated both in phase and out-of-phase, and a phased array of five point sources which simulates the trace velocity of a propeller. The sound field on the exterior surface of the cylinder was measured using a traversing array of 12 microphones. The vibrational response of the structure in the source plane was measured with 22 accelerometers. The interior sound field was measured extensively using an array of six microphones mounted on a computer controlled traversing mechanism. The measured data compares well with previously measured data and acoustic and structural predictions. The data analysis indicate that the sound field is strongly affected by exterior noise source phasing. The presence of damping material on the interior sidewall acts to broaden and reduce the sharp acoustic resonances compared to the untreated interior, as well as reduce the overall sound pressure level transmitted to the interior.

Introduction

The interior noise levels of twin-engine turboprop airplanes, especially the high-speed advanced turboprop airplane, are dominated by the propeller-generated airborne noise transmitted through the fuselage sidewall. The low-frequency spectrum of this noise is very tonal in nature, being dominated by the blade passage frequency and its multiples. The propeller noise, the structural-acoustic transmission paths, and the interior absorption characteristics need to be understood and controlled in order to reduce the interior noise to levels that meet passenger acceptance criteria.

A number of theoretical models have been developed and used to predict the noise radiated from propellers¹ and to predict the resulting interior noise in a realistic aircraft cabin.^{2,3,4,5} These studies of noise transmission have generally

required numerical models that provide little insight to the physical mechanisms inherent in the transmission process. Recent work by Silcox, Lester, and Fuller⁶ has provided insight into these mechanisms and the work of Fuller⁷ has demonstrated the effect of source phasing on the structural-acoustic response of simple fuselage models. More recently, the theoretical work of Silcox and Lester⁸ examined the effect of the source type, location, frequency and distribution on the wave number distribution (modal distribution) of a simple fuselage model.

The application of composite materials to primary and secondary aircraft structures, combined with the high noise levels generated by advanced turboprops, have engendered a need for theoretical and experimental research to examine and describe the acoustic response of this type of aircraft construction. Due primarily to its lighter weight, the noise transmission characteristics of composite fuselage structures are thought to be inferior to traditional aluminum structures. Without a thorough understanding of the noise transmission mechanisms for realistic built-up composite structures, innovative solutions such as passive and active damping and active noise control, cannot be implemented. The purpose of the present paper is to examine the structural-acoustic response of a large scale built-up composite fuselage model and qualitatively compare to that obtained previously from much simpler experimental and analytical models. It is expected that this comparison will guide future work. Towards this end, a number of different exterior noise source configurations were studied over a wide range of frequencies. The exterior pressure distribution was measured using an array of microphones. The structural response of the composite cylinder in the source plane was measured using an array of accelerometers and the interior noise pressure field was mapped using a traversing microphone array.

Experimental Procedure

Test Apparatus Description

In the following sections the major components of the test apparatus, the composite cylinder with stiffeners and floor, the rigid endcaps which shield against airborne noise transmission, and the specific acoustic sound sources, will be described. Figure 1 shows the test apparatus

mounted on a stand in the large anechoic chamber of the Acoustics Research Laboratory at NASA Langley Research Center in Hampton, Virginia. This test configuration provided an environment for a comprehensive mapping of the exterior and interior sound fields in a free field environment. This was an important consideration in order to guarantee a high quality data base for analysis of particular noise transmission characteristics.

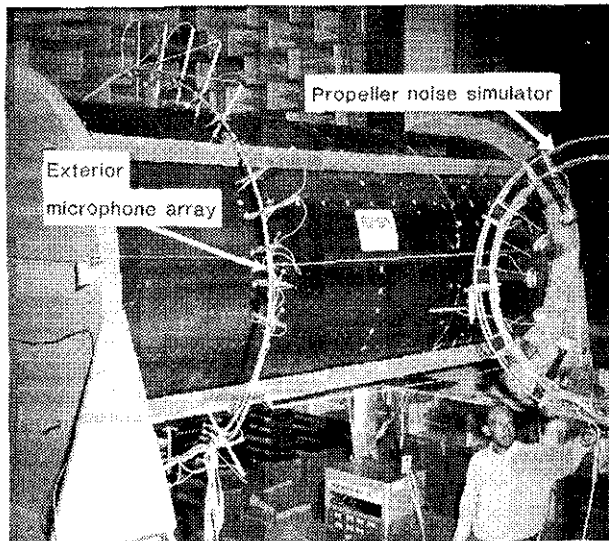


Figure 1. Composite cylinder in anechoic chamber.

Composite Cylinder Fuselage Model.-

The aircraft fuselage model used in the current study is a filament wound, stiffened cylinder 5.5 feet in diameter and 12 feet in length. The composite material of the cylinder shell consists of carbon fibers embedded in an epoxy resin. The ply sequence of the cylinder skin is $\pm 45/\pm 32/90/\mp 32/\mp 45$ for a total thickness of 0.067 inch. The cylinder is stiffened (longitudinally) by 22 evenly spaced composite hat-section stringers. The stringers pass through 10 composite J-section ring frames spaced 15 inches apart. The ring frames and stringers are tied together with a clip and all elements of the fuselage are rivet-bonded together. A schematic of the cylinder cross-section with detail of the stringer-frame geometry is shown in Figure 2. A 0.5 inch thick plywood floor is installed 21.4 inches above the bottom of the cylinder. The supporting beams and posts for the floor are made from aluminum extrusions. An aluminum clip ties the floor to the shell at discrete locations. The plywood floor is bolted to the aluminum supporting beams. Rubber gaskets and silicon rubber sealant fill the gaps between the floor edge and the cylinder structure in order to acoustically isolate the spaces above and below the floor. Additional details of the composite cylinder may be found in Ref. 9.

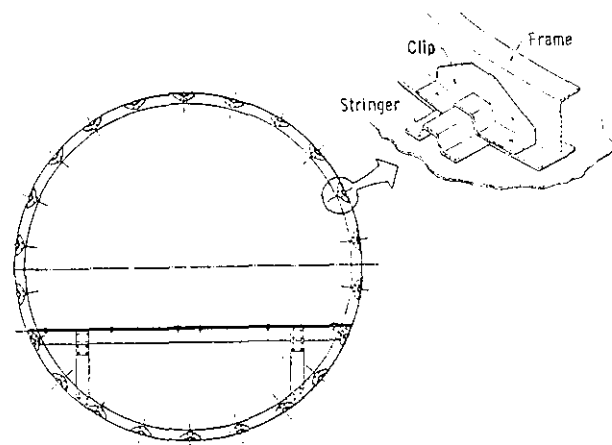


Figure 2. Cross section of composite cylinder.

The cylinder endcaps were constructed from three layers of 1.25 inch thick particle board with a 0.125 inch wide groove cut out for the end of the cylinder to rest in. The endcaps are sufficiently massive so that any airborne sound transmission through them is negligible compared to the sound transmission through the cylinder sidewall. The endcap structure is held in place by four 0.5 inch diameter tension rods. An access door was cut in one of the endcaps, this endcap is usually referred to as the front endcap. Acoustically sealed boxes, installed on the inside and outside of the front endcap, provide connections for microphones and electronic equipment.

Most of the test cases in this study were performed on the bare, untreated cylinder with the floor installed. A series of tests were performed with a simple interior treatment consisting of a 1.0 inch thick acoustic foam damping material placed on the cylinder sidewall between the ring frames. No treatment was placed on the floor or endcaps.

Acoustic Noise Sources.- Three types of acoustic drivers were used for the exterior noise sources. A 16-inch diameter low frequency loudspeaker driving a large vented horn with exit dimensions 32.0 in. x 27.5 in. was used for test frequencies from 60 to 200 Hz. This was used for the very low frequency (VLF) test conditions. A cone driver with a flat oval surface 5.5 in. x 9.0 in. was used for frequencies from 100 to 400 Hz and was called the low frequency (LF) test condition. An electrodynamic driver connected to a small 13 inch long horn with a 0.75 in. x 3.0 in. exit was used to generate frequencies from 400 to 900 Hz. These cases are referred to as the high frequency (HF) test condition. For the frequency ranges selected, the dimensions of the LF and HF drivers are sufficiently small compared to the wavelength of the emanated sound so that the drivers can be considered as point sources. Different tests were run to study the effects of different source configurations. These

source configurations included a single point source located in a plane 1/3 the cylinder length (48 inches) from the front end of the cylinder, and two point sources located in the same plane on opposite sides of the cylinder operated both in phase and out of phase. A specialized noise source configuration consisting of a phased array of five of the small high frequency drivers was used to simulate the trace velocity of a propeller (see Figure 1). This source was operated over the 300 to 800 Hz frequency range. The individual drivers were calibrated to the same amplitude level with a relative phase difference to simulate upswEEP and downswEEP. Many of the tests were repeated with the sources at different radial distances from the cylinder surface (still within the same plane) to study the effects of source location on noise transmission. All of the sources produced exterior sound pressure levels between 100-110 dB over their respective frequency ranges as measured by a reference microphone located at the source.

Instrumentation

For each source configuration in this study the exterior noise field near the cylinder's surface, the surface vibration and the interior noise field were measured. The test matrix shown in Table 1 shows the different conditions analyzed in the current study.

The exterior noise field was sampled with 12 one-half inch condenser microphones mounted normal to the cylinder surface on an aluminum traversing mechanism (see Figure 1). The microphones were positioned approximately 0.5 inch from the cylinder surface. Depending on the source type and location, 9 or 10 longitudinal locations were sampled. Whenever possible, the exterior field was measured in positions corresponding to those cross sections measured in the interior.

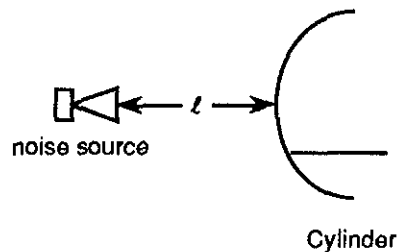
The vibration of the cylinder skin was measured with 22 accelerometers mounted around the cylinder circumference in the source plane (1/3 the cylinder length, 48 inches from the front endcap). After calibration, the accelerometers were attached to the skin with alpha cyanoacrylate adhesive. They were equally spaced around the cylinder circumference opposite the 22 interior longitudinal stiffeners. For a limited number of test cases the accelerometers on one half of the cylinder were removed and repositioned between the remaining accelerometers to yield twice the spatial information on one half of the cylinder.

The sound field transmitted to the interior of the cylinder above the floor was sampled with six equally spaced 0.5 inch condenser microphones mounted on a radial boom. The boom was attached to an automatic traversing mechanism (see Figure 3).

Table 1. Text Matrix for Composite Cylinder Noise Transmission Study

Frequency Range Source Location (<i>l</i>)	Single Source		2 Sources		Phased Array Propeller Simulator
	Untreated	Treated	In-Phase	Out-of-Phase	
60-200 Hz 0.8 a	X				
100-400 Hz 0.2 a	X	X	X	X	
0.4 a	X				
0.8 a	X	X	X	X	
400-900 Hz 0.2 a	X	X	X	X	
0.4 a	X				
0.8 a	X	X	X	X	
1.6 a	X				
300-800 Hz 0.2 a					X
0.8 a					X

a is the cylinder radius = 33 inches



Under computer control, the boom could be positioned at any longitudinal location along the beam and could be rotated through all angles above the floor. Specifically, for each test case, the interior sound field was measured at 8 longitudinal locations (18 in. to 123 in. from the front endcap in 15 inch increments). At each of these longitudinal locations the boom was positioned at 19 azimuthal angles (-108° to +108°, where 0° is vertical up). The interior sound field was thus mapped at 912 points. The amount of time for one cross sectional sweep (19 angles) was approximately 15 minutes, the entire interior space required more than 2 hours to collect the data.

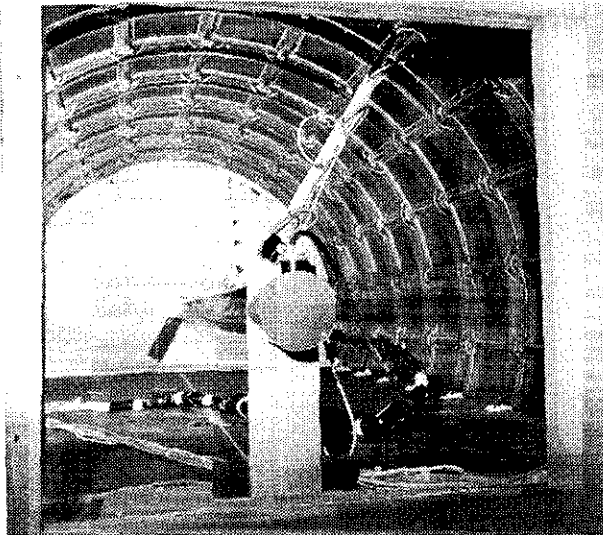


Figure 3. Cylinder interior showing stiffener geometry and microphone boom.

There were three reference microphones: one for each exterior source in use (positioned as close to the source as possible) and one in the cylinder interior. These reference microphones were sampled after each measurement sweep and compared to a spectrum from the beginning of that test case. In this way the source levels could be monitored and maintained at proper levels throughout a test. A test could be aborted when abnormal signal levels were detected. The temperature was measured below the cylinder, inside the cylinder and above the cylinder at the beginning of each test case and after each sweep. Temperatures in the anechoic chamber were maintained at $60^{\circ}\text{F} \pm 1^{\circ}\text{F}$. The temperature inside the cylinder during an interior sweep increased between $1^{\circ}\text{-}2^{\circ}\text{F}$ due to the mechanical heat generated by the stepping motors. A humidity sensor recorded the relative humidity in the anechoic chamber.

Data Acquisition and Reduction

The measured data consists of transfer functions (real and imaginary parts) between the sensors (microphones and accelerometers) and the

exterior source drive signal output from channel A of the analyzer. The signal generated by the analyzer to drive the exterior sources was a pseudo-random signal consisting of 100 equally spaced discrete frequencies over a specified frequency range. For the VLF source these frequencies ranged from 0-200 Hz in 2 Hz steps. For the LF sources the frequencies ranged from 0-400 Hz, every 4 Hz. The HF sources output ranged from 400-900 Hz in 5 Hz steps. The propeller simulator (phased array) contained discrete frequencies every 5 Hz from 300 to 800 Hz with varying phase offsets to simulate upsweep and downsweep. Due to low frequency speaker response characteristics, the usable data for the VLF and LF sources were 60-200 Hz and 100-400 Hz, respectively.

Data from the measurement sensors were fed via a group of multiplexers to channels B, C, and D of the 4 channel analyzer which then acquired three transfer functions with respect to the drive signal from channel A. The transfer functions were comprised of 32 averages and were displayed for operator verification before storage. Data were stored in memory until either a complete exterior mapping, an accelerometer scan, or a single interior cross-section was completed, at which time a file was written to disk. An appropriate calibration factor was determined and set within the analyzer so that the exterior and interior microphone data were stored as complex linear spectra with amplitude normalized to be SPL.

Calibration

As mentioned above, a complete mapping of the interior space of the fuselage model required more than 2 hours of data collection. An entire test case, including both exterior and interior mappings and the accelerometer measurements, often required more than 4 hours to complete. In order to maintain consistent data integrity, the exterior and interior microphones were calibrated at the start of each testing day and whenever a setup modification, such as a new exterior source installation, was required. An appropriate calibration frequency was selected depending on the exterior source type. The VLF and LF source configurations had microphones calibrated to 94 dB at 250 Hz. The propeller simulator and the HF source configurations had microphones calibrated at 94 dB at 500 Hz.

The exterior sound sources also required calibration. Most of the test configurations were straightforward, only requiring an adjustment of the amplifier until the desired output level at a specific frequency was measured by the reference microphone. The two point sources operating in phase and 180° out of phase had separate amplifiers and separate reference microphones. The five HF

drivers in the propeller simulator had to have the same amplitude levels with varying phase shifts in order to simulate upsweep and downsweep.

Discussion of Results

An analysis of some important noise transmission characteristics of the composite fuselage model will be presented in the following paragraphs. Particular attention will be focused on the effects of exterior noise source phasing on dominant interior modes, the interior distributions resulting from varying trace velocities on the exterior, and comparisons of untreated and treated interiors.

Frequency response curves such as those shown in Figures 4 and 5 have been used to examine the general behavior of the interior sound field under different test configurations. These plots were obtained by dividing the complex transfer function of a specific interior microphone, $H_1(int)$, by the complex transfer function of the reference microphone, $H_1(ref)$, located at the exterior source. The interior microphone selected for these plots was on the microphone boom nearest the wall (approximately 2.5 inches from the sidewall), with the boom in the source plane (48 inches from the front endcap) and oriented -84° with respect to vertical, i.e. pointing towards the source. These figures show the level at this particular microphone relative to the respective source level.

Figure 4 shows the interior response for the bare, untreated cylinder and for the cylinder whose sidewall was treated with a 1.0 inch thick foam damping material. A single exterior source was located 0.2 cylinder radius from the cylinder surface for both configurations. The untreated case has little inherent damping so the interior response is highly resonant, as indicated by the numerous sharp peaks in the spectrum. In contrast, the addition of foam damping to the interior sidewall helps broaden the resonances and reduce the overall response, especially evident above 400 Hz. The two spectra are very similar at the lowest frequencies, below 120 Hz, because the acoustic wavelengths are too long for the treatment to have any effect. In general, the interior is dominated by acoustic mode resonances over the plotted frequency range since the addition of treatment causes all frequencies to be reduced. If there were some dominant structural modes driving an off resonant acoustic response, there would be common peaks in both spectra because the foam damping would not strongly affect their behavior.

The interior frequency response for two different exterior source configurations is shown in Figure 5. The solid line represents the interior response due to two exterior sources operated in-phase located on opposite sides of the cylinder in a plane 48 inches from the front endcap. The

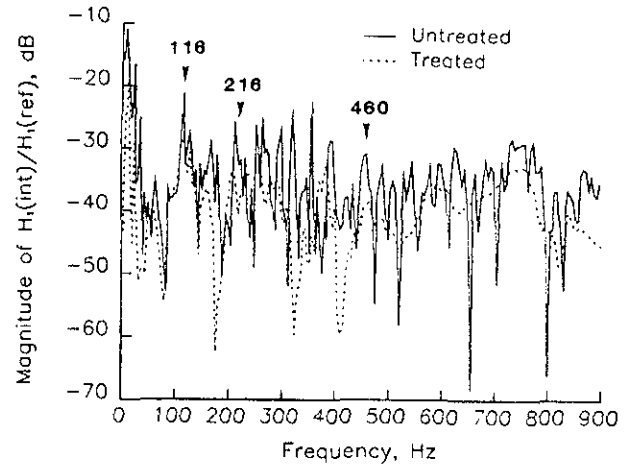


Figure 4. Frequency response of interior microphone nearest sidewall. Microphone boom oriented at -84° . Single exterior source at $\ell=0.2a$.

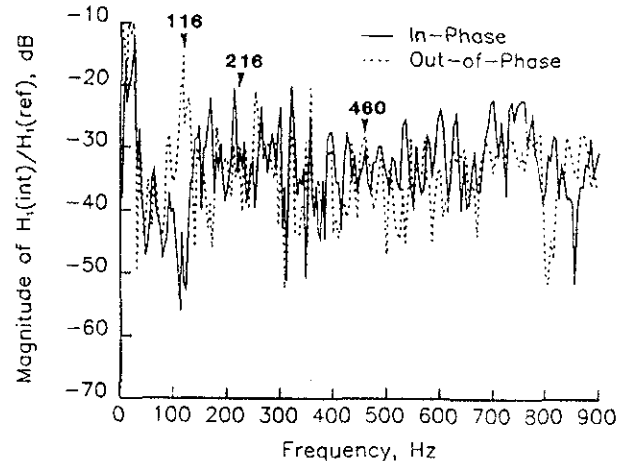


Figure 5. Frequency response of interior microphone nearest sidewall. Microphone boom oriented at -84° . Two exterior sources at $\ell=0.2a$ operated in-phase and 180° out-of-phase.

sources are 0.2 cylinder radius from the cylinder surface. When the same sources are operated out-of-phase, the interior response is that indicated by the dashed curve. As in Figure 4, the sharp peaks across the frequency range indicate a strong resonant response in the interior for both in-phase and out-of-phase configurations. Close examination of Figure 5 reveals that the response at some frequencies is enhanced by one phase configuration but reduced by the other. Two of these frequencies, 116 Hz and 216 Hz, will be examined below using actual interior noise distributions extracted from the interior pressure field survey.

Very Low Frequency Response

Figure 6 shows a shaded contour plot that represents the interior noise distribution at 46 Hz due to the VLF exterior source located 48 inches from the front endcap and 0.8 cylinder radius from the outside shell wall. The darker shades of gray represent lower sound pressure levels. The range of SPL is indicated on the scale in the middle of the figure. This frequency was selected because it agrees well with the first acoustic cavity mode predicted at 46.8 Hz using the PAIN model. Also, since the composite cylinder approximates a half-scale model of typical tilt-rotor aircraft, the cylinder's response at 46 Hz may correspond to that of the tilt-rotor at its fundamental blade passage frequency between 20-25 Hz. The circular cross section (top of figure) in the source plane shows a weak response with a maximum at 0° or vertical that drops off 8-10 dB near the floor at ±108°. Because this frequency is too low to couple with any of the interior cross-sectional modes, it has a high transmission loss. The longitudinal cross section (bottom of figure) shows the interior noise distribution between 18" and 123" from the front endcap when the microphone boom was oriented vertically at 0°. The arrow indicates the axial location of the exterior source. The contour plot reveals maximum levels at the ends and a nodal minimum approximately in the center. Since the wavelength at 46 Hz in air is almost 24 feet, one-half wavelength exactly fits the cylinder's longitudinal dimension of 12 feet. This is the first acoustic cavity mode of the composite cylinder.

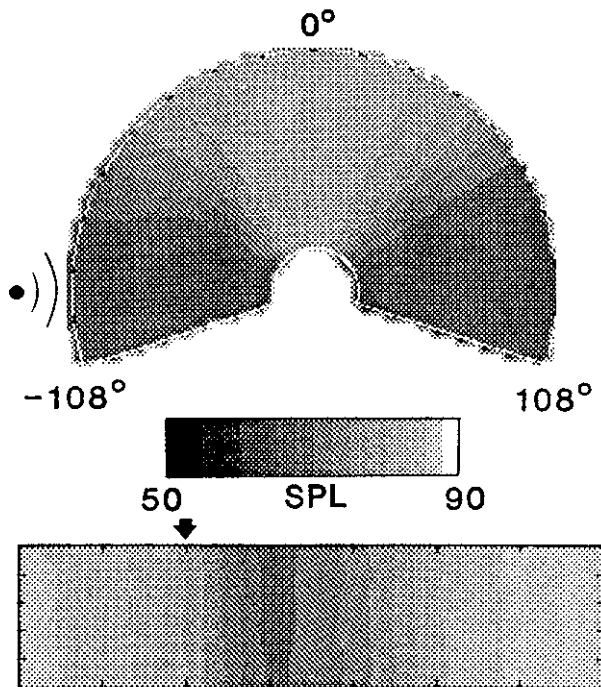


Figure 6. Interior response at 46 Hz due to VLF exterior source located at $\ell=0.8a$. Longitudinal cross section at 0°.

Effects of Source Phasing on Interior Modal Response

Figures 7a and 7b show the response of the interior at 116 Hz due to two LF exterior sources located 0.2 cylinder radius from the cylinder's surface on opposite sides of the cylinder operated out-of-phase and in-phase, respectively. Each figure shows the distribution in a circular cross section above the floor in the source plane and a longitudinal cross section where the microphone boom was oriented -84° with respect to vertical. The dominant modal response in the circular cross section has a nodal line along the vertical centerline. This is an odd, or antisymmetric mode. There is little variation in the amplitude distribution along the longitudinal cross section. Figure 7a illustrates how this odd mode is reinforced when the two sources are operated 180° out-of-phase, coupling strongly into the antisymmetric characteristics of the mode. However, when the sources are operated in-phase, the peak sound pressure levels in the interior drop over 10 dB and the modal behavior is forced away from a clear antisymmetric distribution (see Figure 7b). The circular cross section indicates a weakly symmetric response with two radial nodal lines. The non-uniform longitudinal distribution is an indication that other cavity modes are being forced that have non-uniform axial distributions.

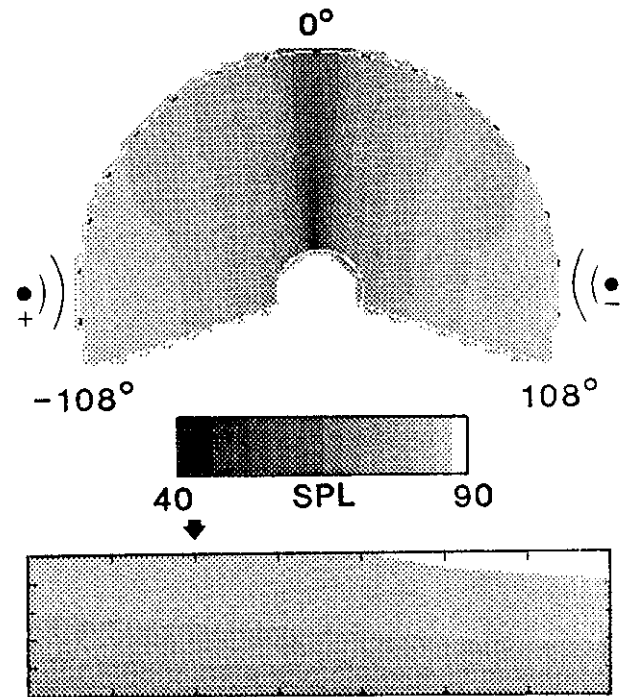


Figure 7a. Interior response at 116 Hz. Two LF exterior sources at $\ell=0.2a$ operated 180° out-of-phase. Longitudinal cross section at -84°.

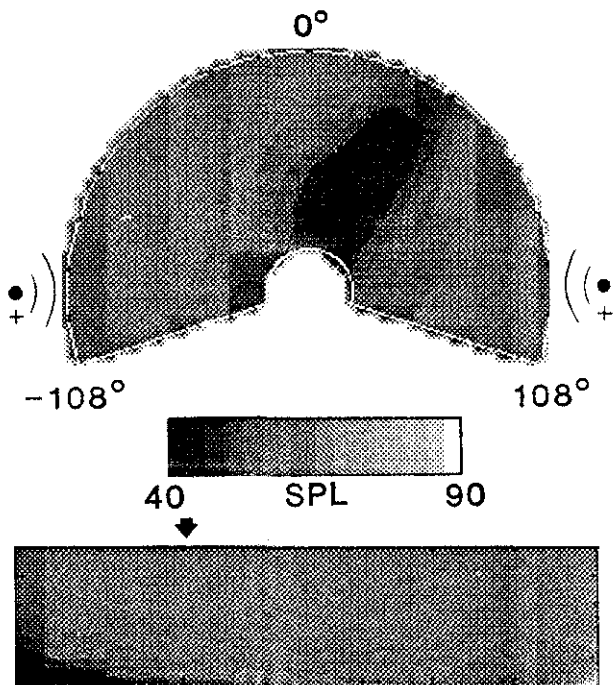


Figure 7b. Interior response at 116 Hz. Two LF exterior sources at $\ell=0.2a$ operated in-phase. Longitudinal cross section at -84° .

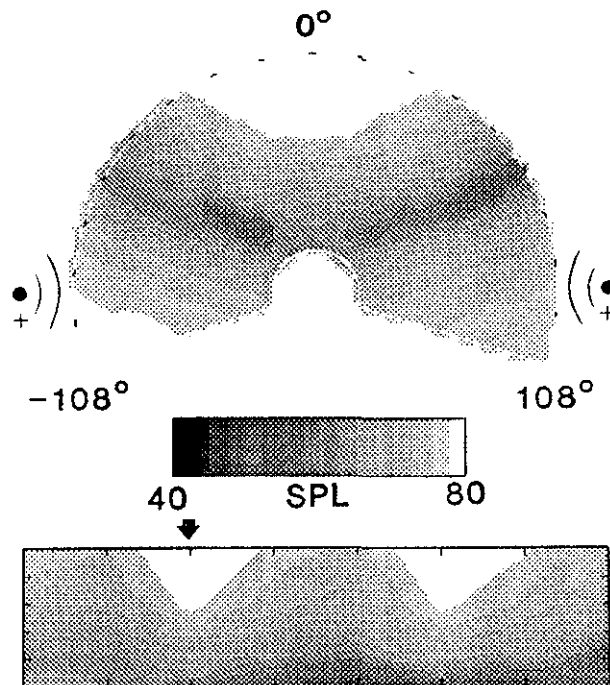


Figure 8a. Interior response 216 Hz. Two LF exterior sources at $\ell=0.2a$ operated in-phase. Longitudinal cross section at 0° .

Figures 8a and 8b show the response of the interior at 216 Hz for the same two exterior source configurations as above. Here the response in the circular cross section is dominated by an even mode (symmetric with respect to the vertical). Note that the peak levels in the circular cross section do not occur opposite either source but at the vertical. The axial response has a clear $\cos(2\pi x/L)$ behavior, as shown in the longitudinal cross section where the microphone boom was oriented vertically. At this frequency the effects of exterior noise source phasing are just the opposite. Figure 8a illustrates how the in-phase exterior sources reinforce the even mode in both the circular and longitudinal cross sections. When the sources are operated 180° out-of-phase, the modal behavior in the circular cross section is forced away from a symmetric distribution and the peak levels drop by more than 10 dB (Figure 8b).

Effects of Source Location on Interior Noise

Figure 9a and 9b show the interior response at 116 Hz and 216 Hz, respectively, for the same source configurations illustrated in Figures 7a and 8a except that the sources are 0.8 cylinder radius from the cylinder surface. The antisymmetric response shown in the circular cross section in Figure 9a is again reinforced by the out-of-phase exterior sources, but the peak sound pressure level is down almost 4 dB from that seen in Figure 7a. The

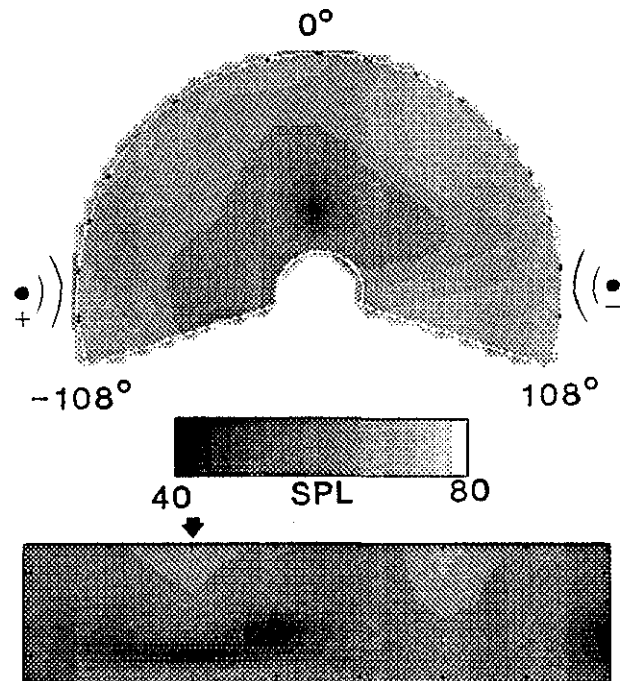


Figure 8b. Interior response at 216 Hz. Two LF exterior sources at $\ell=0.2a$ operated 180° out-of-phase. Longitudinal cross section at 0° .

longitudinal cross section shown in Figure 9a is also reduced in level and is slightly more uniform because the increased source separation creates a more

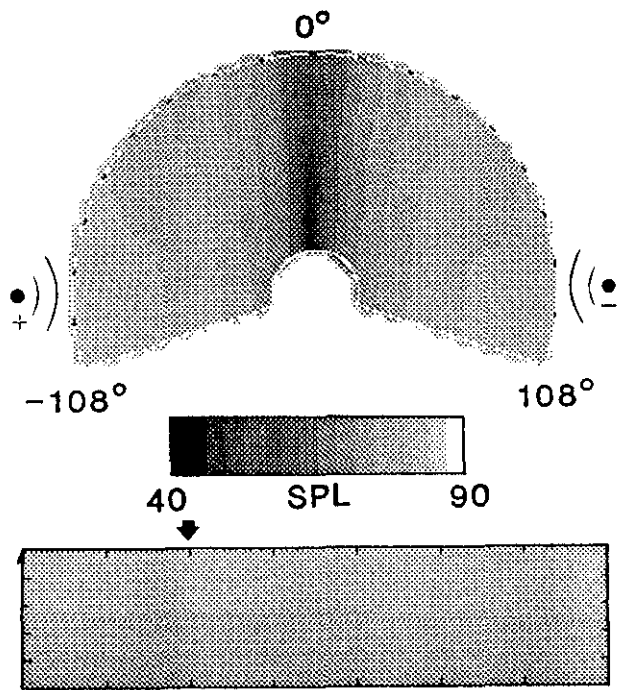


Figure 9a. Interior response at 116 Hz. Two LF exterior sources at $\ell=0.8a$ operated 180° out-of-phase. Longitudinal cross section at -84° .

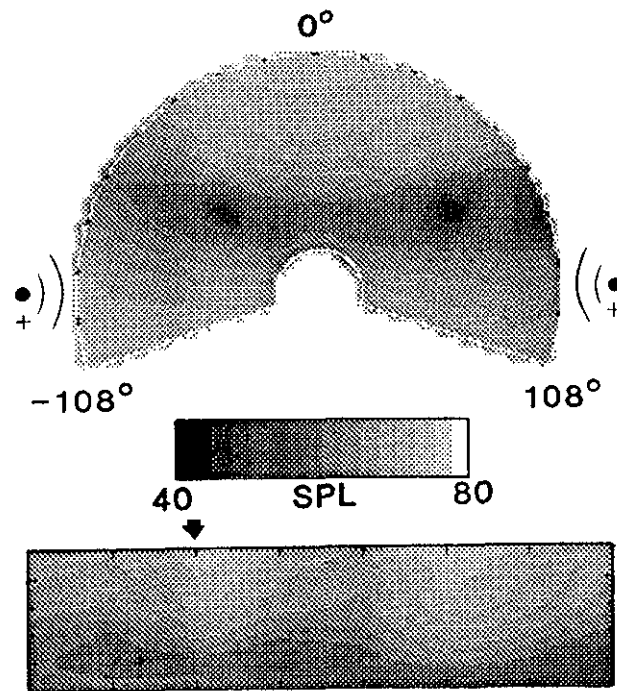


Figure 9b. Interior response at 216 Hz. Two LF exterior sources at $\ell=0.8a$ operated in-phase. Longitudinal cross section at 0° .

distributed exterior excitation. The interior response for the even mode at 216 Hz is similarly affected by increased exterior source separation. The symmetric response in the circular cross section and the

$\cos(2\pi x/L)$ behavior in the longitudinal cross section seen in Figure 8a are still evident in Figure 9b, but the peak sound pressure levels are down almost 7 dB.

Effects of Exterior Trace Velocity on Transmitted Noise

Another mechanism of noise transmission which can be analyzed using the current experimental data base concerns the effects of exterior trace velocity on transmitted interior noise. Figure 10a shows the interior noise distribution at 460 Hz due to a single HF source located 0.2 cylinder radius from the cylinder surface. Figure 10b shows the interior noise distribution at 460 Hz when the exterior source produces a trace velocity on the surface. This is the five-source phased array simulating propeller upsweep. The closest driver is 0.2 cylinder radius from the surface. The circular cross section is in the source plane. The microphone boom was oriented at -84° (towards source) for the longitudinal cross section.

Although the dominant modal behavior is not as clear as in some of the previous lower frequency cases, there are still some important points that can be made. Comparing Figures 10a and 10b, the general modal order in the circular cross section is retained when the cylinder is excited by the five-source phased array. However, due to the trace velocity imparted by the phased array, the antinode of the interior pressure response (indicated by asterisk) has rotated downward. This effect is predicted by the analytical model in reference 7. The peak levels in Figure 10b occur at $\pm 10^\circ$ instead of at -82° as seen in Figure 10a. This may be due to a stronger modal coupling for the five-source phased array as indicated by the more clearly defined mode structure in Figure 10b. For the single source, the longitudinal response shows a local hot spot adjacent to the exterior source. The cause of the localized minimum in Figure 10a is not clear considering the otherwise uniformity in this plane. The more uniform longitudinal response of the five-source phased array (Figure 10b) can be attributed to the more distributed field on the exterior.

Effects of Interior Treatment

The final area of noise transmission mechanisms to be addressed in this paper concerns the effects of sidewall treatment on interior noise distributions. Figures 11a and 11b show the interior response of the bare, untreated cylinder and the response when a 1.0 inch thick acoustic foam damping material was installed on the interior sidewall between the ring frames. Both test cases used a single LF exterior source at 216 Hz located 0.2 cylinder radius from the surface. As expected, the

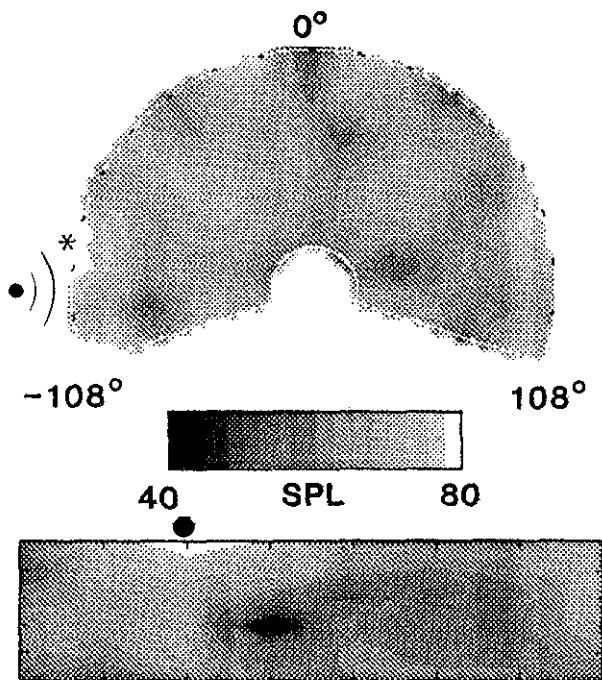


Figure 10a. Interior response 460 Hz due to a single HF exterior source at $\ell=0.2a$. Longitudinal cross section -84° .

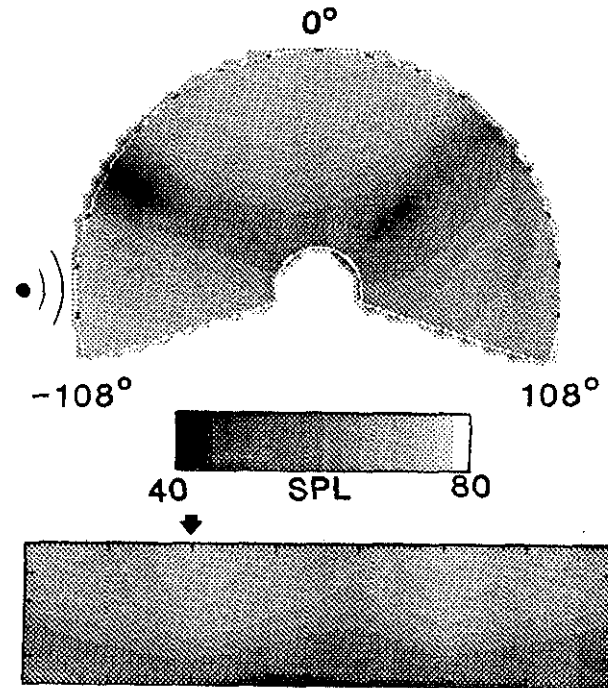


Figure 11a. Interior response at 216 Hz due to a single LF exterior source at $\ell=0.2a$. Longitudinal cross section at 0° . Untreated interior.

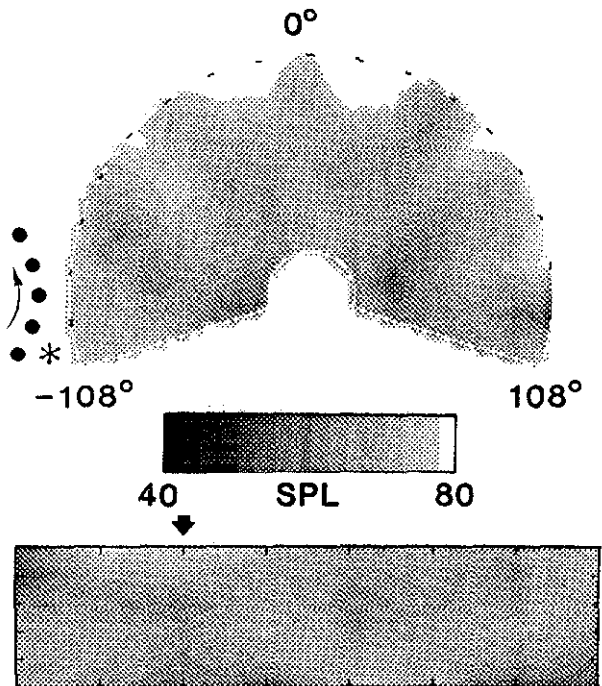


Figure 10b. Interior response at 460 Hz. Five-source phase array at $\ell=0.2a$ operated in upswep mode. Longitudinal cross section at -84° .

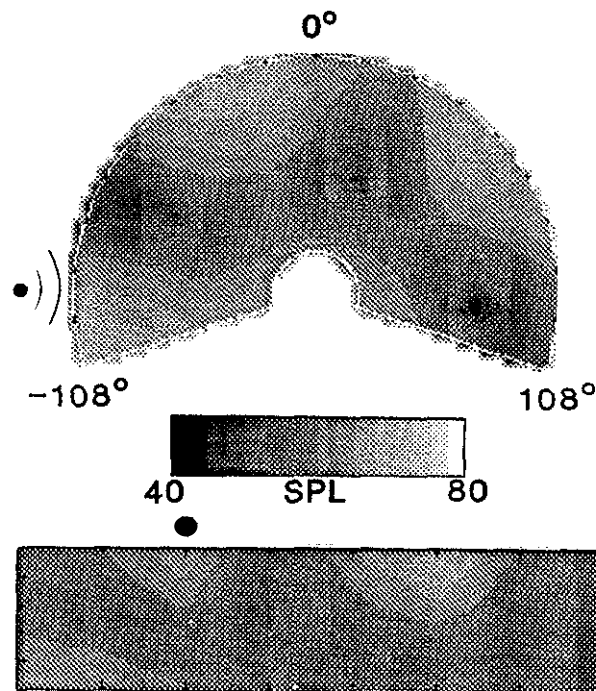


Figure 11b. Interior response at 216 Hz due to a single LF exterior source at $\ell=0.2a$. Longitudinal cross section at 0° . Interior sidewall treated with 1.0 inch thick foam.

sections. As seen in the spectra in Figure 4, the addition of the foam causes the acoustic resonance at 216 Hz to broaden and damp the level so that other acoustic modes compete and affect the actual interior noise distribution (Figure 11b).

peak sound pressure level in the treated interior has been reduced (approximately 4 dB). More interesting, however, is the apparent shift in modal behavior in both the circular and longitudinal cross

Concluding Remarks

This paper has described some of the initial findings from an experimental test undertaken to study the basic noise transmission characteristics of a realistic, built-up composite fuselage model. The floor-equipped stiffened composite cylinder was exposed to several different exterior noise source configurations in a large anechoic chamber. These exterior source configurations included a single point source, two point sources located in the same plane on opposite sides of the cylinder, and a propeller simulator. The results indicate that the interior source field is strongly affected by exterior noise source phasing. Some modes are reinforced while other are reduced. The primary effect of exterior source location is a reduction in levels in the interior, the dominant modal behavior remains the same. The general modal behavior due to the five-source phased array is similar to that from a single exterior source but is shifted towards the region of increased exterior excitation. The presence of sidewall treatment was shown to reduce the overall interior sound pressure levels and dampen dominant acoustic resonances so that other acoustic modes can affect the interior noise distribution. Additional analysis of the data is required to more fully understand some of these noise transmission mechanisms. Future work will correlate the measured exterior sound fields to the vibrational response of the cylinder and the resulting interior acoustic response. Comparisons of measured data to appropriate analytical prediction models are being pursued.

References

- ¹Farassat, F.: Linear Acoustic Formulas for Calculation of Rotating Blade Noise. *AIAA Journal*, Vol. 19, 1981, pp. 1122-1130.
- ²Pope, L. D.; Wilby, E. G.; and Wilby, J. F.: Propeller Aircraft Interior Noise Model. NASA 3813, July 1984.
- ³Grosveld, F. W.; Sullivan, B. M.; and Marulo, F.: Aircraft Interior Noise Prediction Using a Structural-Acoustic Analogy in NASTRAN Modal Synthesis. Proceedings of the 6th International Modal Analysis Conference, Orlando, FL, February 1-4, 1988, pp. 1191-1198.
- ⁴Cheng, C. Y. R.; and Seybert, A. F.: Recent Applications of the Boundary Element Method to Problems in Acoustics. Proceedings of SAE Noise and Vibration Conference, Traverse City, MI, 1987, pp. 389-398.
- ⁵Bullmore, A. J.: A Comparison of Single Analytical Models for Representing Propeller Aircraft Structural and Acoustic Response. ISVR Technical Report no. 153, University of Southampton, February 1988.
- ⁶Silcox, R. J.; Fuller, C. R.; and Lester, H. C.: Mechanisms of Active Control in Cylindrical Fuselage Structures. *AIAA Journal*, August 1990.
- ⁷Fuller, C. R.: Analytical Investigation of Synchrophasing as a Means of Reducing Aircraft Interior Noise. NASA CR 3823, August 1984.
- ⁸Silcox, R. J.; and Lester, H. C.: Propeller Modelling Effects on Interior Noise in Cylindrical Cavities with Application to Active Control. Presented at the 1989 Aeroacoustics Conference.
- ⁹Jackson, A. C.; Balena, F. J.; La Barge, W. L.; Pie, G.; Pitman, W. A.; and Wittlin, G.: Transport Composite Fuselage Technology — Impact Dynamics and Acoustic Transmission. NASA CR 4035, December 1986.